Submitted to ADVANCED MATERIALS

Supporting Information for:

Single Continuous Wave Laser Induced Photodynamic/Plasmonic Photothermal Therapy Using Photosensitizer-Functionalized Gold Nanostars

Shouju Wang, Peng Huang, Liming Nie, Ruijun Xing, Dingbin Liu, Zhe Wang, Jing Lin, Shouhui Chen, Gang Niu, Guangming Lu, and Xiaoyuan Chen**

Experimental Section

Materials

$HAuCl_4 \cdot 3H_2O$, $AgNO_3$, sodium citrate, ascorbic acid, N-(3-dimethylaminopropyl)-N'-ethylcarbodiimide hydrochloride (EDC), N-hydroxysulfosuccinimide sodium salt (sulfo-NHS), triethylamine (TEA), dimethylformamide (DMF), thiazolyl blue tetrazolium bromide (MTT), dimethyl sulphoxide (DMSO) were purchased from Sigma-Aldrich (St. Louis, MO). Sodium azide was purchased from Acros organics (Geel, Belgium). Chlorin e6 (Ce6) was purchased from Froniter Scientific, Inc. (Logan, UT). Thiol-PEG-amine ($HS\text{-}PEG\text{-}NH_2$, M.W. ≈ 2000 Da) was purchased from Nanocs, Inc (New York, NY). Singlet oxygen sensor green (SOSG) and LIVE/DEAD viability/cytotoxicity kit were purchased from Invitrogen (Grand Island, NY). All chemicals were analytical grade and used without further purification.

A549 (lung cancer) and MDA-MB-435 (breast cancer) lines were obtained from the American Type Culture Collection (Manassas, VA). A549 cells were kept at 37°C and 5% CO_2 in DMEM media (Cellgro, Manassas, VA) supplemented with 10% fetal bovine serum (Invitrogen) while MDA-MB-435 were incubated in L-15 media (Cellgro) supplemented with 10% fetal bovine serum (Invitrogen).

Preparation of GNS-PEG

GNS-PEG was prepared by a seed-mediated method. Typically, the seed solution was prepared by adding 3 mL of 1% sodium citrate solution to 100 mL of boiling 1.0 mM $HAuCl_4$ solution under vigorous stirring. Then 50 μL of cooled citrate-stabilized seed solution was added to 10 mL of 0.25 mM $HAuCl_4$ solution; Next, 40 μL of 0.01 M $AgNO_3$ and 50 μL of 0.1 M ascorbic acid were added simultaneously. The solution was stirred until its color turned from light red to dark blue. After that, 10 μL of 10 mM HS-PEG-NH_2 solution was added. The reaction mixture was kept under stirring at room temperature for 2 h.

Preparation of GNS-PEG-Ce6

Covalent binding of Ce6 to the GNS-PEG was performed using a modification of the standard EDC-NHS reaction. Briefly, prepared GNS-PEG solution was centrifuged at 3, 500 rcf for 15 min and decanted to remove excess HS-PEG-NH_2. The GNS-PEG pallets were suspended in DMF. To activate the carboxylic group of Ce6, Ce6, NHS, EDC, and TEA were dissolved in DMF in molar ratio of about 1:1.2:1.2:3 under vigorous stirring for 30 min. Then activated Ce6 was added into GNS-PEG solution to react with the amine group of GNS-PEG. After that,

the solution was centrifuged, decanted and suspended in ultra pure water or PBS for further characterization and application.

Characterization of GNS-PEG-Ce6

The morphology of samples was recorded in a Tecnai TF30 TEM (FEI, Hillsboro, OR) equipped with a Gatan Ultrascan 1000 CCD camera (Gatan, Pleasaton, CA). Hydrodynamic diameter and Zeta potential were measured by a SZ-100 nano particle analyzer (HORIBA Scientific, Tokyo, Japan). The gold concentration in solution was determined by a JY2000 Ultrace ICP S2 Atomic Emission Spectrometer (HORIBA). The corresponding concentration of GNS-PEG-Ce6 particles was calculated by a sphere model of 55 nm diameter. UV-Vis spectra was measured by a Genesys 10S UV-Vis spectrophotometer (Thermo Scientific, Waltham, MA). The absorbance at 404 nm was used as a marker for the successful conjugation of Ce6. To estimate the amount of Ce6 conjugated on each GNS, the GNS-PEG-Ce6 was collected by centrifugation, the unconjugated Ce6 in the supernatant was quantified by using Ce6 UV calibration curve at 404 nm (Figure S3b). Fluorescence intensity was monitored with an F-7000 fluorescence spectrophotometer (Hitachi, Tokyo, Japan). Singlet oxygen was detected by SOSG following manufacturer's instructions. Thermal images were captured by a SC300 infrared camera (FLIR, Arlington, VA) and processed with Examin IR image software (FLIR). The excitation source was a 671 nm diode-pumped solid-state laser system (LASERGLOW Technologies, Toronto, Canada).

Fluorescence Imaging of Cellular Uptake

MDA-MB-435 cells were plated at least 24 h before incubation with GNS-PEG-Ce6 in LabTek II coverglass (Nalge Nunc Internationl, Rochester, NY) at a density of 5×10^4 cells/mL and grown to 60-80% confluence. The cells were incubated with 0.875 nM GNS-PEG, 0.875 nM GNS-PEG-Ce6 (corresponding to 5 μM Ce6) or 5 μM free Ce6 and incubated for 24 h. After incubation, the cells were thoroughly washed twice with PBS. Images were acquired by an IX81 motorized inverted microscope (Olympus, Hamburg, Germany). The fluorescence micrographs shown are representative of at least three independent experiments. Individual cell profiles from microscopy images were processed for fluorescence intensity using ImageJ (NIH, Bethesda, MD).

Quantitative Analysis of Cellular Uptake

MDA-MB-435 cells were incubated with 0.875 μM GNS-PEG, 0.875 μM GNS-PEG-Ce6 (corresponding to 5 μM Ce6) or 5 μM free Ce6 for 24 h. After rinsing twice with PBS, the cells were collected by Accuir C6 flow cytometer using CFlow Plus software (BD, Ann Arbor, MI). All data was analyzed using 10,000 cells by FlowJo version 7.6.5 (FlowJo, Ashland, OR).

***In vivo* Fluorescence Imaging of GNS-PEG-Ce6**

Tumor-bearing mice were prepared by subcutaneously injecting a suspension of 5×10^6 MDA-MB-435 cells in PBS (100 μL) into bilateral shoulders of female nude mice (six weeks old, 20-25g). When the tumor size reached ~60 mm^3, 50 μL of 17.5 nM GNS-PEG-Ce6 (corresponding to 100 μM Ce6) was intratumorally injected into the tumor-bearing mice.

Fluorescence imaging was performed with a Maestro all-optical imaging system (Caliper Life Sciences, Hopkinton, MA) at 4 h post-injection. The Ce6 spectrum was unmixed from autofluorescence by Maestro 2 software (Caliper Life Sciences).

***In vivo* Thermal Imaging**

When the tumor size reached ~60 mm^3, 50 μL of 17.5 nM GNS-PEG-Ce6 (corresponding to 100 μM Ce6), 17.5 nM GNS-PEG, or 100 μM Ce6 was intratumorally injected into the tumor-bearing mice. Thermal Imaging was recorded by a SC300 infrared camera (FLIR) when the tumors were exposed to 671 nm laser (LASERGLOW Technologies) of power density at 0.25 W/cm^2, 0.5 W/cm^2, or 1.0 W/cm^2.

***In vivo* Photoacoustic Imaging**

When the tumor size reached ~60 mm^3, 50 μL of PBS, 17.5 nM GNS-PEG-Ce6 (corresponding to 100 μM Ce6), 17.5 nM GNS-PEG, or 100 μM Ce6 was intratumorally injected into the tumor-bearing mice. Photoacoustic (PA) imaging was performed by a Vevo 2100 LAZR system (VisualSonics Inc. New York, NY) equipped with a 40 MHz, 256-element linear array transducer on tumors after 671 nm laser irradiation (1.0W/cm^2, 6 min). The PA excitation source was an optical parametric oscillator (OPO) laser (tunable 680-970 nm, 20 Hz repetition rate, 5 ns pulse width, ~20 mJ pulse energy) pumped by doubled Nd:YAG laser. To generate maximum ultrasound transients, the tumors were positioned ~8 mm under the ultrasound transducer to acquire both PA and ultrasound images. Capitalizing on the distinct difference in the absorption spectra between oxyhemoglobin (HbO2) and

deoxyhemoglobin (HbR), two excitation wavelengths (750 and 850 nm) were used to estimate the concentrations of HbO2 and HbR. The average fractional oxygen saturation inside tumors was mapped by Matlab software (ver. 2012b).

***In vivo* Phototoxicity Study**

When the tumor size reached ~60 mm^3, MDA-MB-435 tumor-bearing mice were divided into 7 groups. Mice in group 1, 2 and 3 received an intratumoral injection of 50 μL of 17.5 nM GNS-PEG-Ce6 (6 tumors each group), 17.5 nM GNS-PEG (6 tumors each group) or 100 μM free Ce6 (6 tumors each group), followed by 6 min of laser irradiation at 1.0 W/cm^2 at 4 h post-injection. In parallel studies, mice in group 4, 5 and 6 received an intratumoral injection of 50 μL of 17.5 nM GNS-PEG-Ce6 (4 tumors each group), 17.5 nM GNS-PEG (4 tumors each group) or 100 μM free Ce6 (4 tumors each group), with no laser irradiation. As control group, mice in group 7 received an intratumoral injection of 50 μL PBS (4 tumors), followed by 6 min of laser irradiation at 1.0 W/cm^2. The tumor sizes were measured by caliper every two days after treatment.

***Ex vivo* Histological Staining**

Tumors were dissected from MDA-MB-435 tumor-bearing mice on day 8 after treatment, fixed in a 4% formaldehyde solution for 10 min at room temperature, and embedded in OCT medium (Miles Inc, Elkhart, IN). The tumors were frozen and sections (10 μm in thickness) were cut on a cryostat. Haematoxylin and eosin (H&E) staining (BBC Biochemical, Mount

Vernon, WA) was performed following manufacturer's instructions and observed by a BX41 brightfield microscopy (Olympus).

Statistical Analysis

Difference among the groups tested was determined by one-way ANOVA and TukeyHSD post hoc testing. Significance level was set at $P<0.05$.

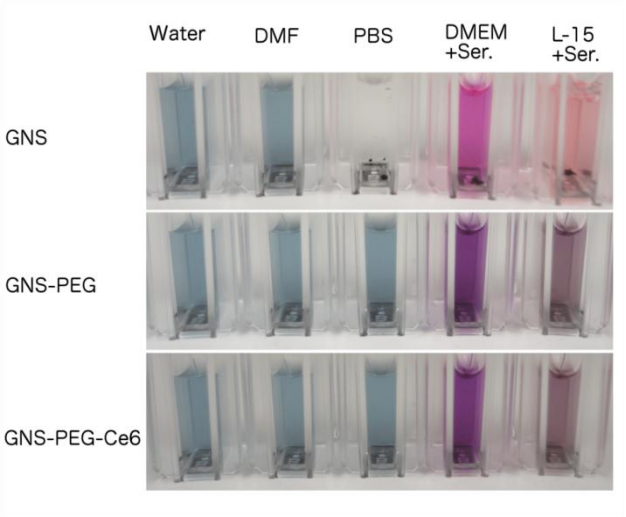

Figure S1. Photographs of GNS, GNS-PEG and GNS-PEG-Ce6 in various solutions including ultra pure water, DMF, PBS, DMEM with 10% FBS and L-15 media with 10% FBS. Both GNS-PEG and GNS-PEG-Ce6 showed excellent stability in physical solutions without noticeable aggregation.

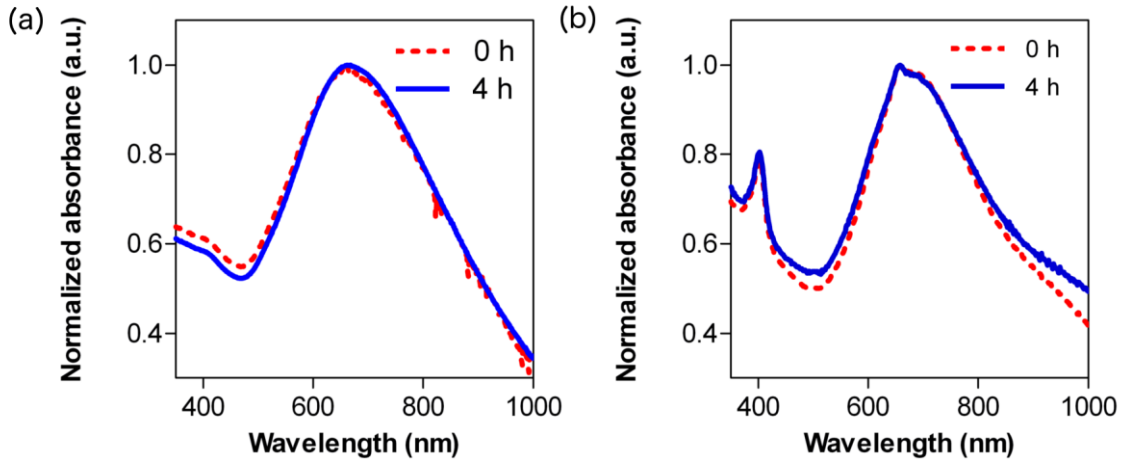

Figure S2. Normalized UV-Vis spectra of (a) GNS-PEG and (b) GNS-PEG-Ce6 dispersed in PBS with 10% fetal bovine serum immediately and after 4 h.

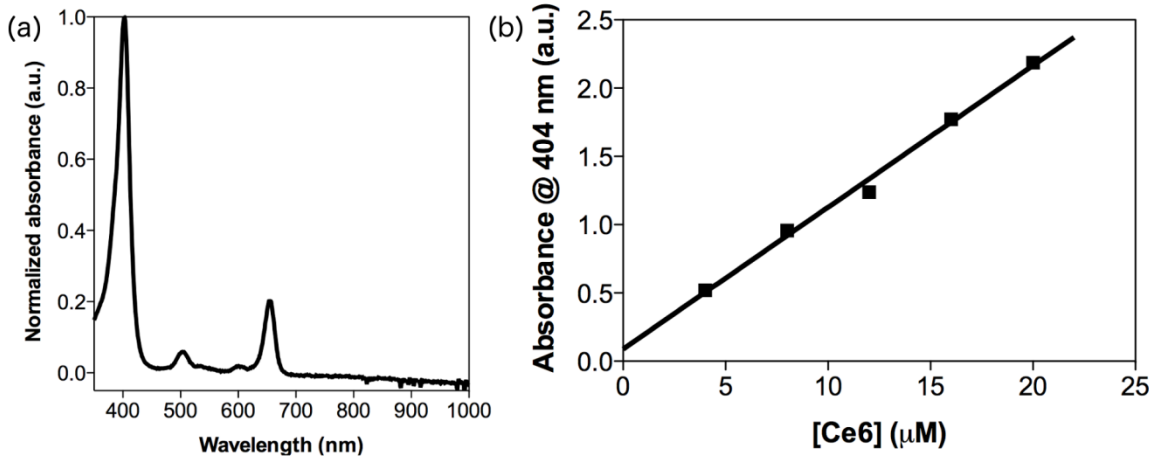

Figure S3. (a) Normalized UV-Vis spectra of Ce6 dispersed in PBS. (b) The linear relationship between concentration and absorbance of Ce6 at 404 nm.

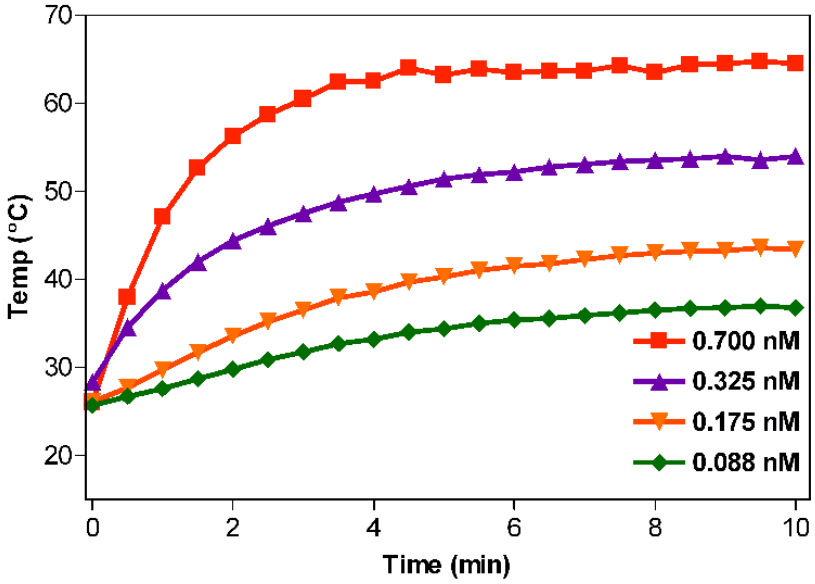

Figure S4. Temperature of GNS-PEG-Ce6 at various concentrations upon 671 nm laser irradiation (2.0 W/cm^2) over time.

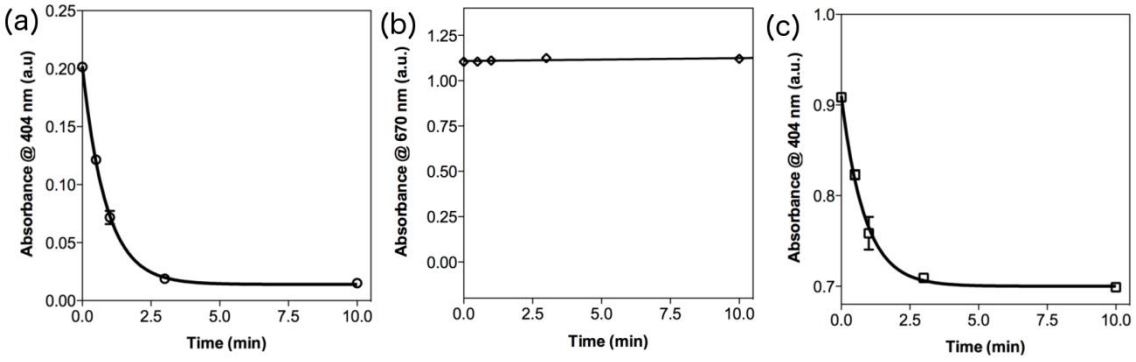

Figure S5. The change of absorbance of (a) Ce6 at 404 nm, (b) GNS-PEG at 670 nm, (c) GNS-PEG-Ce6 at 404 nm upon 671 nm laser irradiation (2.0 W/cm^2) over time.

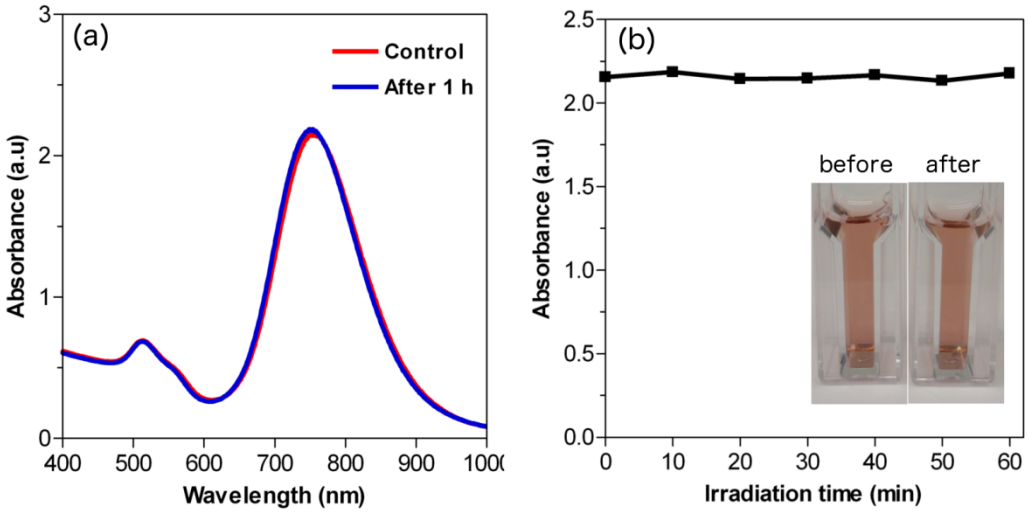

Figure S6. (a) UV-Vis spectra of gold nanorods before and after 1 h CW laser irradiation (808 nm, 2.0 W/cm^2). (b) The change of absorbance of gold nanorods at 770 nm under laser irradiation over time. Inserts are photographs of gold nanorods before and after irradiation. Gold nanorods exhibited great photostability under CW laser irradiation.

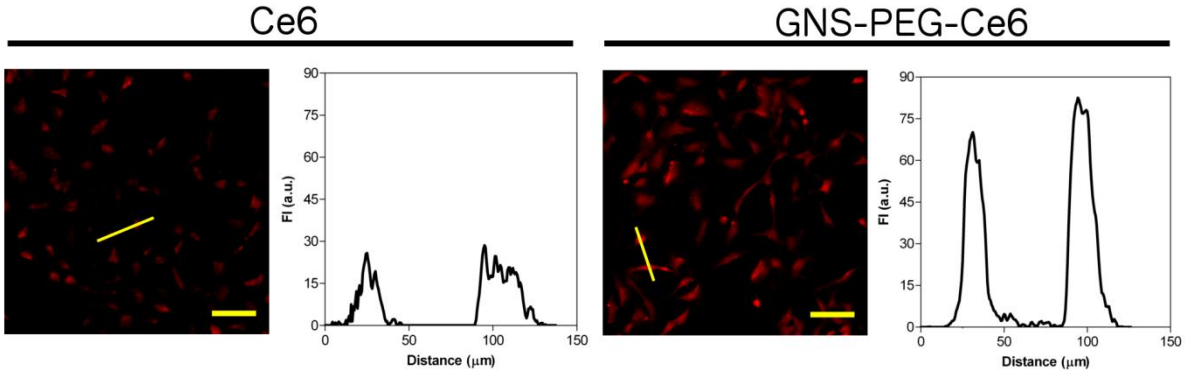

Figure S7. Fluorescence images and intensity profiles of MDA-MB-435 cells incubated with 5 μM of free Ce6 or 0.875 nM of GNS-PEG-Ce6 (corresponding to 5 μM of free Ce6) for 24 h.

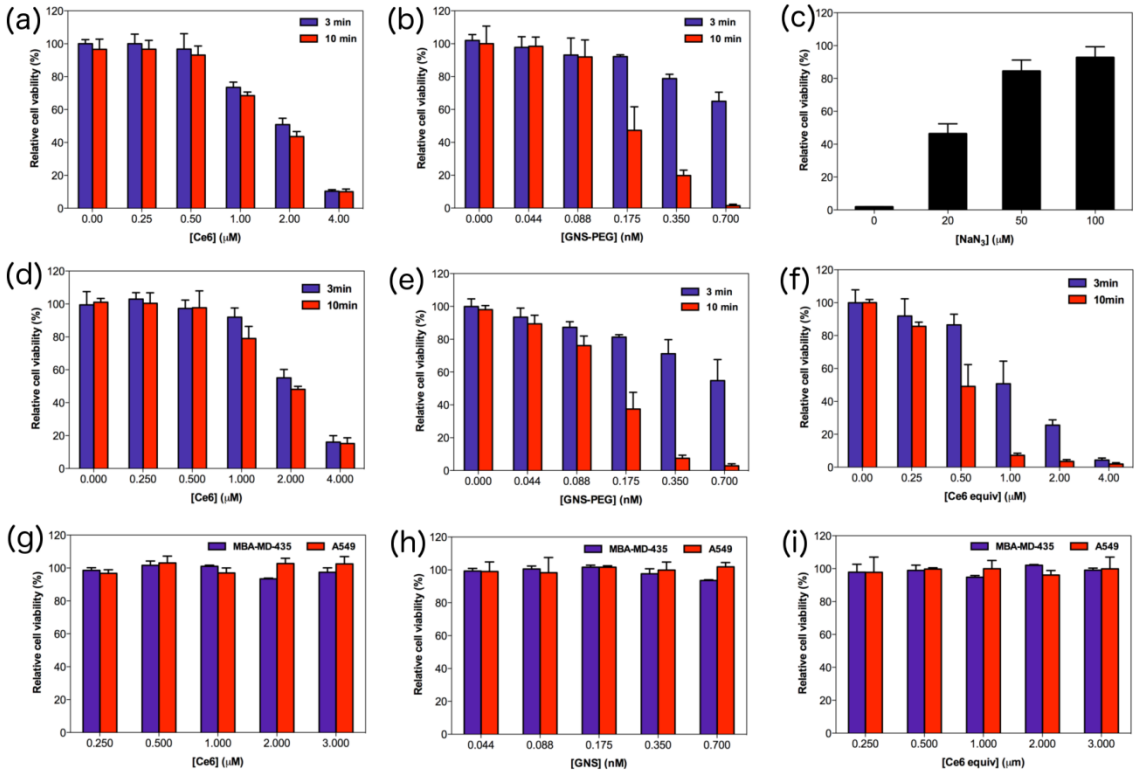

Figure S8. Relative cell viability of MDA-MB-435 cells incubated with different concentration of (a) free Ce6 or (b) GNS-PEG for 24 h followed by 671 nm laser irradiation (2.0 W/cm^2) for 3 min or 10 min. (c) Relative cell viability of MDA-MB-435 cells incubated with 10 μM free Ce6 with presence of various concentration of NaN3 followed by 671 nm laser irradiation (2.0 W/cm^2) for 10 min. Relative cell viability of A549 cells incubated with different concentration of (d) free Ce6, (e) GNS-PEG, (f) GNS-PEG-Ce6 for 24 h followed by 671 nm laser irradiation (2.0 W/cm^2) for 3 min or 10 min. Relative cell viability of MDA-MB-435 and A549 cells incubated with different concentration of (g) free Ce6 (h) GNS-PEG or (i) GNS-PEG-Ce6 without laser irradiation.

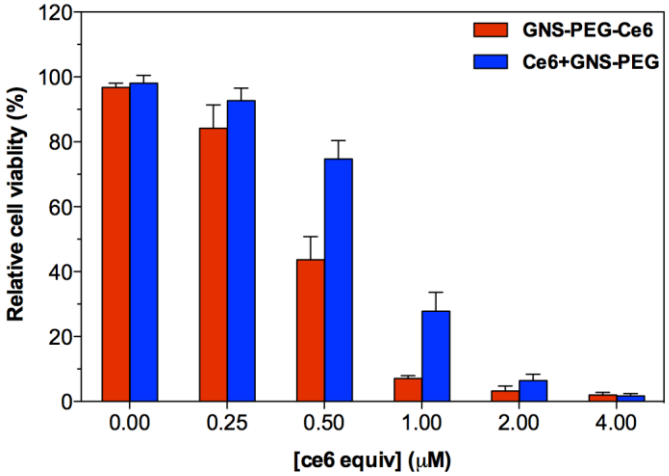

Figure S9. Relative cell viability of MBA-MD-435 cells incubated with GNS-PEG-Ce6 or the same concentration of mixture of free Ce6 and GNS-PEG for 24 h followed by 671 nm laser irradiation (2.0 W/cm^2) for 10 min.

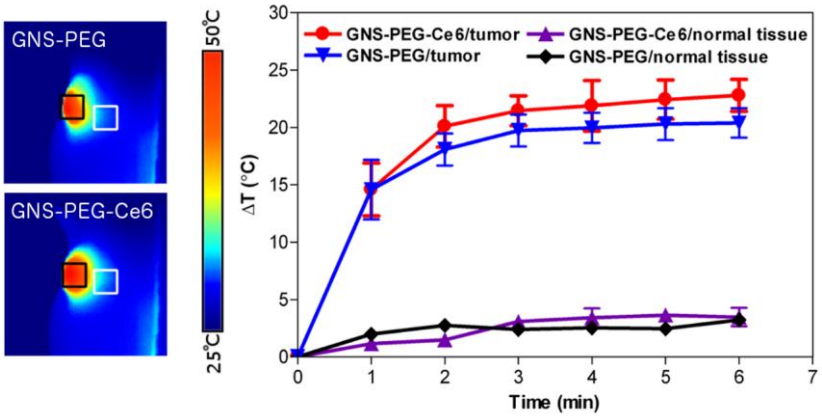

Figure S10. Heating curves of tumors and surrounding normal tissues upon 671 nm laser irradiation over time after injection of GNS-PEG and GNS-PEG-Ce6. The black squares indicate the location of tumors. The white squares indicate the location of surrounding normal tissues.

Dear Dr. Kalveram,

Thank you for your and the two Reviewers' efforts in the review of our manuscript entitled "Single Continuous Wave Laser Induced Photodynamic/Plasmonic Photothermal Therapy Using Photosensitizer-Functionalized Gold Nanostars" for consideration as a communication paper in Advanced Materials. Both Reviewers gave us very constructive comments and suggestions, which have helped us to improve our manuscript. Both Reviewers asked for minor revisions.

The point-by-point responses to the comments from the Reviewer 1 are listed as follows,

1) The author suggests that the ce6-conjugated nanostar displays improved in vivo therapeutic effect than the modalities alone, however they are missing the free-ce6 + gold nanostar control. This treatment group will allow the authors to determine if the synergistic effect of the two-treatment modality is dependent on the conjugation of the two components.

Re: According to the reviewer's important suggestion, we compared the therapeutic effect of GNS-PEG-Ce6 with free Ce6 + GNS-PEG by MTT assay. The result was described in Page 12, "It's interesting that GNS-PEG-Ce6 showed higher therapeutic effect than the mixture of free Ce6 and GNS-PEG at the same concentration, which can be attributed to the enhanced cellular uptake efficiency of Ce6 after conjugation with GNS-PEG (Figure S9)."

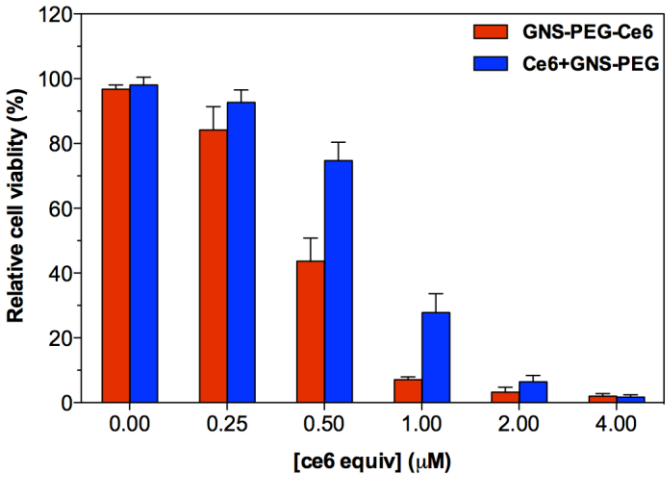

Figure S9. Relative cell viability of MBA-MD-435 cells incubated with GNS-PEG-Ce6 or the same concentration of mixture of free Ce6 and GNS-PEG for 24 h followed by 671 nm laser irradiation (2.0 W/cm^2) for 10 min.

Since the free-Ce6 + gold nanostar exhibits lower therapeutic effect than GNS-PEG-Ce6 in vitro, we reasoned that the synergistic effect of the dual-modality treatment is dependent on the conjugation of Ce6 and GNS-PEG. Furthermore, the conjugation of these two components allows the co-localization of PDT and PTT effects in vivo.

2) The stability study does not probe the influence of time on the modification of the gold nanostars. The authors examine a single timepoint using photographic imaging, and contend that no aggregation occurs. However, this experiment does not test at longer timepoints and hence, limits the conclusions that can be made about the particles storage and serum stability. Furthermore, aggregation can occur at a nanoscale level which is not observed by visually inspecting the solution by eye and instead should be examined by spectroscopy. The 4 hour timepoint is especially important since it will inform the authors of whether the particle was still intact at 4 hours post intratumor injection.

Re: According to the reviewer's helpful suggestion, we measured the UV-Vis spectrum of GNS-PEG and GNS-PEG-Ce6 in PBS with 10% fetal bovine serum immediately and after 4 h incubation. No obvious changes of spectra were observed in GNS-PEG and GNS-PEG-Ce6 solutions, indicating the excellent serum stability of these two nano-conjugates. We described that in page 5, "The UV-Vis spectra showed that GNS-PEG and GNS-PEG-Ce6 were extremely stable in PBS with 10% serum (Figure S2)."

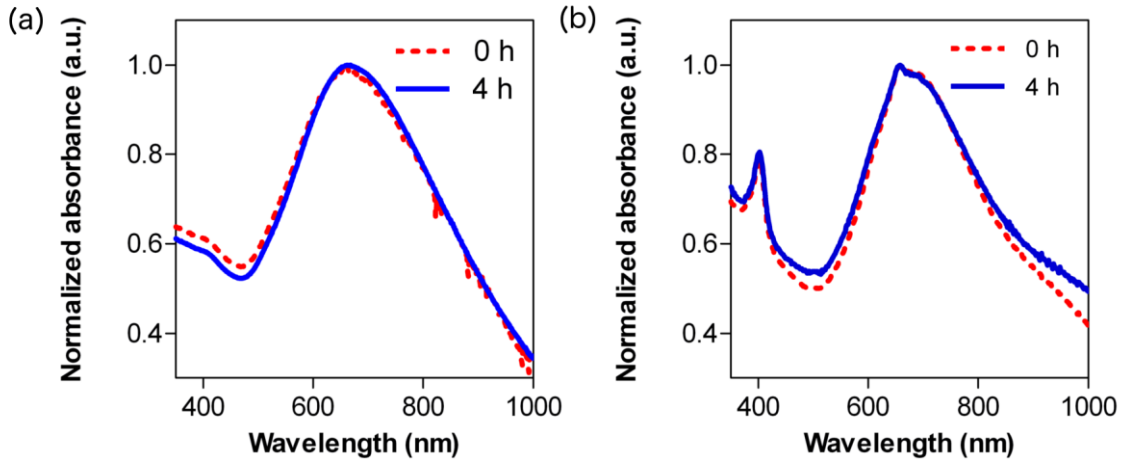

Figure S2. Normalized UV-Vis spectra of (a) GNS-PEG and (b) GNS-PEG-Ce6 dispersed in PBS with 10% fetal bovine serum immediately and after 4 h.

3) The fluence used for in vivo treatment is not reflective of a typical PDT fluence and hence could artificially compound the hypoxic effect by PDT (Lasers Surg Med, 2006, 38(5), pp 489-93). The authors should conduct the study at a lower fluence to maximize the beneficial PDT effects.

Re: Thanks for the kind reminder. We chose the fluence rate at 1W/cm^2 for in vivo treatment because:

a) The laser used in this study is purposed to excite both PDT and PTT effect upon single excitation. The typical fluence rate for PTT treatment in vivo varies from 0.25 W/cm^2 to 10 W/cm^2 (*Adv. Mater. 2012, 24, pp 5586–5592, J. Am. Chem. Soc. 2006, 128, pp 2115-2120*). The fluence rate we chose is close to the minimum power density reported in PTT treatment, indicating the high heat conversion efficacy of Ce6-conjugated gold nanostars. Since the change of temperature in tumor is positively correlated with fluence rate, lower fluence rate will impede the PTT effects, thus hindering the synergistic therapeutic effect of GNS-PEG-Ce6.
b) PDT damage is dependent on the total light dose (*Photochem Photobiol, 1987, 46(5), pp 837–847*). Lower fluence rate will unavoidably prolong the irradiation time, which is unfavorable in the clinic. At the fluence rate we chose in this study, the significant hypoxic effects were observed in both Ce6 and GNS-PEG-Ce6 treated groups by photoacoustic imaging. This result suggested that PDT treatment was efficient at this fluence rate in our study.

The point-by-point responses to the comments from the Reviewer 2 are listed as follows,

1.(P.5)

The authors showed the amount of Ce6 molecules on GNS using IPC-MS and UV-vis spectrum. However, the absorption of GNS is overlapped with that of Ce6 at 400 nm. For this reason, the author should provide detailed information on the calculation method in the manuscript. Perhaps, gold nanostars should be dissolved or Ce6 molecules should be detached from the GNS to obtain the exact quantity of Ce6 molecules.

Re: According to this important suggestion, we described the calculation method in detail in Page 22-23, **"**To estimate the amount of Ce6 conjugated on each GNS, the GNS-PEG-Ce6 was collected by centrifugation, the unconjugated Ce6 in the supernatant was quantified by using Ce6 UV calibration curve at 404 nm (Figure S3b)."

2.(P.7)

Explain why Ce6 on the surface of GNS produced less amount of the singlet oxygen compared with free Ce6. Other study showed that singlet oxygen quantum yield increased 50 % (Photochem. Photobiol. Sci. 5 (2006), 727-734)

Re: Thanks for the helpful suggestion. In GNS-PEG-Ce6, the laser energy given was absorbed by Ce6 and gold nanostars separately to produce singlet oxygen and heat. Since part of the laser energy was converted into heat, the laser energy for the production of singlet oxygen was less in GNS-PEG-Ce6 than that in free Ce6. Therefore, the Ce6 on the surface of GNS produced less amount of singlet oxygen compared with free Ce6 at the same concentration. Similar results were reported in previous PDT/PTT dual-modality therapy studies (*ACS Nano, 2011, 5(9), pp 7000-7009, ACS Nano, 2011, 5(2), pp 1086-1094*).

In the mentioned paper (Photochem Photobiol Sci, 2006, 5, pp 727-734), the increased quantum yield was "due to the presence of an associated phase transfer agent (tetraoctylammonium bromide; TOAB) which increases the triplet energy transfer". This agent was not used in our study.

3.(P.11-12, 15)
Explain how 17.5 nM of GNS-PEG-Ce6 is equivalent to 100 uM of Ce6. The same amount of Ce6 does not necessarily mean that they have the same therapeutic effect because production of singlet oxygen by Ce6 is different even though there are equal molar number of Ce6 in both GNS-PEG-Ce6 and free Ce6.

In addition, the author should explain how PTT and PDT of GNS-PEG-Ce6 contributed to therapy. (for example, PTT : PDT = 00 % : 00 %)

Re: We appreciate this important comment. It's true that the equal molar number of Ce6 does not necessarily mean that they can produce the same amount of singlet oxygen by GNS-PEG-Ce6 as that by free Ce6. However, the production of singlet oxygen is influenced by local oxygen supply, which is hard to control both in vitro and in vivo. Based on this fact, the amount of singlet oxygen is not a good reference for comparing therapeutic effect of PDT. In contrast, standardizing the amount of photosensitizer is generally accepted in previous related work (*ACS Nano, 2011, 5(9), pp 7000-7009, ACS Nano, 2011, 5(2), pp 1086-1094, ACS Nano, 2012, 6(9), pp 8030-8040*).

To separate individual effects from the synergistic effect, we calculated the ratio of PTT : PDT by equation (1).

$$PTT : PDT = (100\% - RCV_{GNS\text{-}PEG}) : (RCV_{GNS\text{-}PEG} - RCV_{GNS\text{-}PEG\text{-}Ce6}) \quad (1)$$

RCV means relative cellular viability. The result is listed as follows:

[Ce6 equiv.] (μM)	**PTT:PDT**

0.25	2%:14%
0.50	9%:48%
1.00	53%:41%
2.00	80%:17%
4.00	99%:1%

4.(P.12)

The authors administered nanoparticles intratumorally. Therefore, it could cause misunderstanding when they said "A strong uniformly distributed fluorescence signal was observed in the whole tumor." This expression is meaningful only when they did systemic injection. Revise this sentence to indicate that the fluorescence signal was observed in the tumor region for 4 h.

Re: According to the reviewer's advice, we revised this sentence in Page 13, "A strong fluorescence signal was observed in the tumor region within 4 h after injection (Figure 4a)."

5.(P.13)

If the authors wanted to assert that their GNS-PEG-Ce6 has the "tumor selectivity" of PPTT, then they should have shown that the temperature of normal tissues did not increase in spite of GNS-PEG-Ce6 injection followed by laser irradiation.

Re: Thanks for the reviewer's helpful suggestion. We analyzed the change of temperature in the tumor and surrounding normal tissues after GNS-PEG and GNS-PEG-Ce6 injection followed by laser irradiation. The result was described in page 13, "The surrounding healthy tissue showed a moderate increase to 35 – 40 °C. No significant temperature change was observed in other parts of the mouse (Figure S10)."

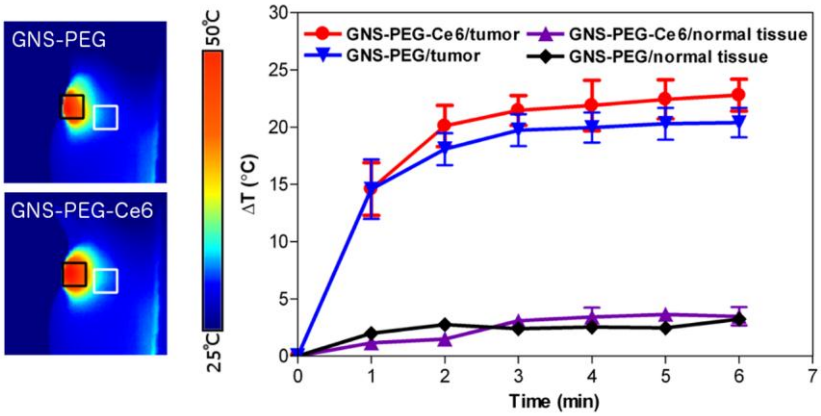

Figure S10. Heating curves of tumors and surrounding normal tissues upon 671 nm laser irradiation over time after injection of GNS-PEG and GNS-PEG-Ce6. The black squares indicate the location of tumors. The white squares indicate the location of surrounding normal tissues.

We marked all changes in red in the revised manuscript.

Thank you once again for your kind consideration.

Sincerely

Xiaoyuan (Shawn) Chen
NIBIB/NIH